COMPUTER METHODS IN MATERIALS SCIENCE

2021, vol. 21, no. 2, 63–74
https://doi.org/10.7494/cmms.2021.2.0746

Optimization of material distribution for forged automotive components using hybrid optimization techniques

Przemysław Sebastjan, Wacław Kuś*

Silesian University of Technology, Department of Computational Mechanics and Engineering, Konarskiego 18A, Gliwice, Poland.

Abstract

The paper deals with the problem of optimal material distribution inside the provided design area. Optimization based on deterministic and stochastic algorithms is used to obtain the best result on the basis of the proposed objective function and constraints. The optimization of the shock absorber is used as an example of the described methods. One of the main difficulties addressed is the manufacturability of the optimized part intended for the forging process. Additionally, nonlinear buckling simulation with the use of the finite element method is used to solve the misuse case of shock absorber compression, where the shape of the optimized part has a key role in the total strength of the automotive damper. All of that, together with the required design precision, creates the nontrivial constrained optimization problem solved using the parametric, implicit geometry representation and a combination of stochastic and deterministic algorithms used with parallel design processing. Two methods of optimization are examined and compared in terms of the total amount of function calls, final design mass, and feasibility of the resultant design. Also, the amount of parameters used for the implicit geometry representation is greatly reduced compared to existing schemes presented in the literature. The problem addressed in this article is strongly inspired by the actual industrial example of the mass minimization process, but it is more focused on the actual manufacturability of the resultant component and admissible solving time. Commercially accessible software combined with authors' procedures is used to resolve the material distribution task, which makes the proposed method universal and easily adapted to other fields of the optimization of mechanical elements.

Keywords: shape optimization, hybrid optimization, genetic algorithms, evolutionary algorithms, gradient algorithms, automotive part optimization

1. Introduction

The optimal material distribution over a fixed design area is one of the most rapidly developing fields of structural mechanics. It aims to allocate material as efficiently as possible so that the structure can be made at minimum cost (weight, area, length, price, etc.), and all the design constraints are met, including the manufacturing restrictions when appropriate. There are dozens of well-described procedures already available in the literature, but they are mostly focused on topology optimization problems, while some of the manufacturing conditions are not included as a scope of the optimization. Special care must be taken when manufacturing-related conditions need to be satisfied. There are works (Li et al., 2015) that present the methodology used for extruded designs optimization, for optimization when minimum or maximum member size is relevant (Zhou et al., 2001), where 3D printed design is created as a result of optimization (Ntintakis et al., 2020). Examples of the implementation of different manufacturing constraints, guaranteeing the feasibility of the resultant design, are described in the works of Vatanabe et al. (2016).

* Corresponding author: waclaw.kus@polsl.pl
ORCID ID's: 0000-0002-5335-8984 (P. Sebastjan), 0000-0001-7616-6881 (W. Kuś)

Nonetheless, all of the above methods are used for obtaining the satisfactory shape of the optimized part, but methods used to drive the optimization process are different among most of the works. Different authors use stochastic (Hu et al., 2014) and deterministic algorithms (Wang & Wang, 2006), local and global search attitudes, or a combination of the above (Hongwen et al., 2017). The choice of the method is critical not only for the efficiency of the optimization (i.e., the final shape itself), but also for the number of function calls or finding local/global extrema.

The work presented in this paper is related to the unstable behavior of automotive shock absorbers when subjected to severe compression loadings, such as running over a curb with high velocity or braking in the pothole. Methods dedicated to solving buckling problems in general already exist in the literature (Ferrari & Sigmund, 2020), but they are rarely convenient or precise enough to capture the actual buckling behavior of the considered chassis structure. That is why the authors decided to use the nonlinear buckling simulations, employing the finite element static strength analysis, to solve the problem of abuse compression loading. The simulated structural behavior is a result of the mutual interaction between the loaded bodies, as well as the change of the load redistribution while severe deformations are achieved.

2. Problem description

The analyzed case concerns the optimization of material distribution (shape optimization) of the forged component – the bottom bracket, which is a part of the automotive shock absorber, as presented in Figure 1. The design area, where material can be allocated, is a space extracted from the chassis kinematic analysis. An example of such geometry is presented in the aforementioned Figure 1 with grey color – however, for the Finite Element Method (FEM) modeling convenience, this area has been already smoothed in order to ease the meshing process and to get rid of the "artificial" stress concentrations. However, the mass of the resultant body is still much higher than expected, therefore the need for the mass (and shape) optimization arises.

As the brackets structural behavior strongly affects the strain and stress distribution of the neighboring components (i.e., the tube and the piston rod, etc.), the structural response of the whole assembly should be used for the optimization of the material allocation. The ultimate goal is to achieve the feasible shape of the bracket, with the lowest possible mass, which is still able to resist the applied compression force without losing stability.

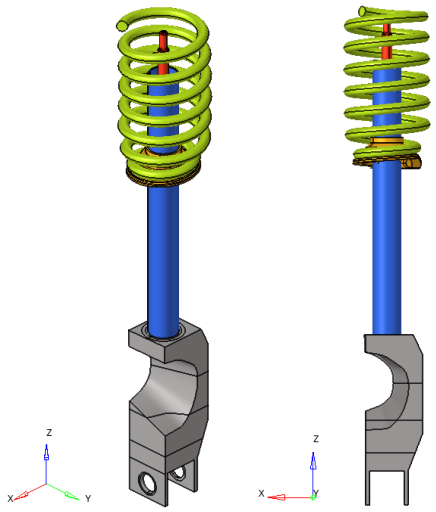

Fig. 1. The geometry of the analyzed shock absorber. The optimized part (the bracket) is marked with grey color and a rectangular window

In this case, an additional problem occurs, as the failure mode is not necessarily located in the bracket itself – the tube can also be the weakest link of the structure. By "failure mode" it is meant, that some part of the structure achieves severe plastic deformation, therefore prevents the structure from resisting increasing load magnitude. The brackets role is not only to support the tube vertically or to allow the shock absorber to be mounted in the chassis (i.e., to the swingarm bushing), but also to provide sufficient lateral stiffness to prevent the radial movement of the tube axis (or simply bending the tube). The reason for that is when the whole structure deflects laterally, the compression load vector is being shifted from the supports, creating the bending moment, which in consequence raise the stress level in the considered parts, as presented in Figure 2 – it can be referred to as eccentric compression.

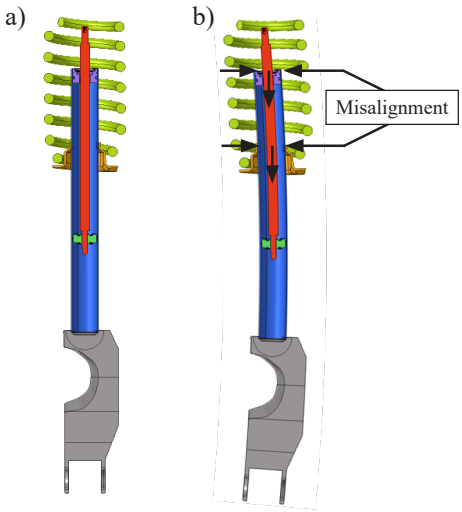

Fig. 2. The cross-sectional view of the shock absorber in: a) the base state; b) under the misuse compression load

There is a certain load level which the shock absorber must withstand, and below which the buckling behavior is forbidden, as presented schematically in Figure 3. Using the maximum resultant reaction force as the constrained value, the following optimization problem is formulated:

Objective function *f*:

$$f(KV_1, KV_2, ..., KV_N) = \rho \int_V dV \rightarrow minimize \quad (1)$$

Constraint *q*:

$$g(KV_1, KV_2, ..., KV_N) = F_{ULTIMATE} \geq F_{LIMIT} \quad (2)$$

where: KV_n – weight assigned to the *n*-th interpolation node, knot value; ρ – material density; V – the volume of the part; $F_{ULTIMATE}$ – maximum force achieved by the shock absorber before losing stability; F_{LIMIT} – required minimum force below which buckling cannot occur.

In order to simulate the structural behavior of the considered shock absorber, the finite element method was used. The nonlinear, static strength analysis was performed in each iteration of the optimization process. The design area covered over 75% of all finite elements used in the analysis, which (for the second-order tetrahedron elements) resulted in almost 200,000 degrees of freedom.

3. Materials and methods

3.1. Optimization methods

The proposed optimization problem is solved using a modified level-set-based method, with radial basis functions for the auxiliary field interpolation. The total number of design parameters is greatly reduced compared to the methods available in the literature (Guirguis & Aly, 2016) even for much smaller problem sizes, but no shape derivatives are calculated (there is no sensitivity calculation) during the optimization process. Such an attitude is a result of two different reasons, shape derivatives are based on gradient methods, which tend to drive the optimization process to reach the local optimum. Additionally, gradient-based methods need to be initiated from a feasible starting point which is not known upfront. Reduced-parameters level set method can be used together with stochastic algorithms in which randomness is incorporated.

The first of the above features is the actual root-cause why the most popular homogenization or one of two similar methods: SIMP – Solid Isotropic Material with Penalization (Bendsøe, 1989) or RAMP – Rational Approximation of Material Properties (Stolpe & Svanberg, 2001) methods were not used to solve the problem. During the design modification (using these methods), convergence was lost due to sudden structural stability issues.

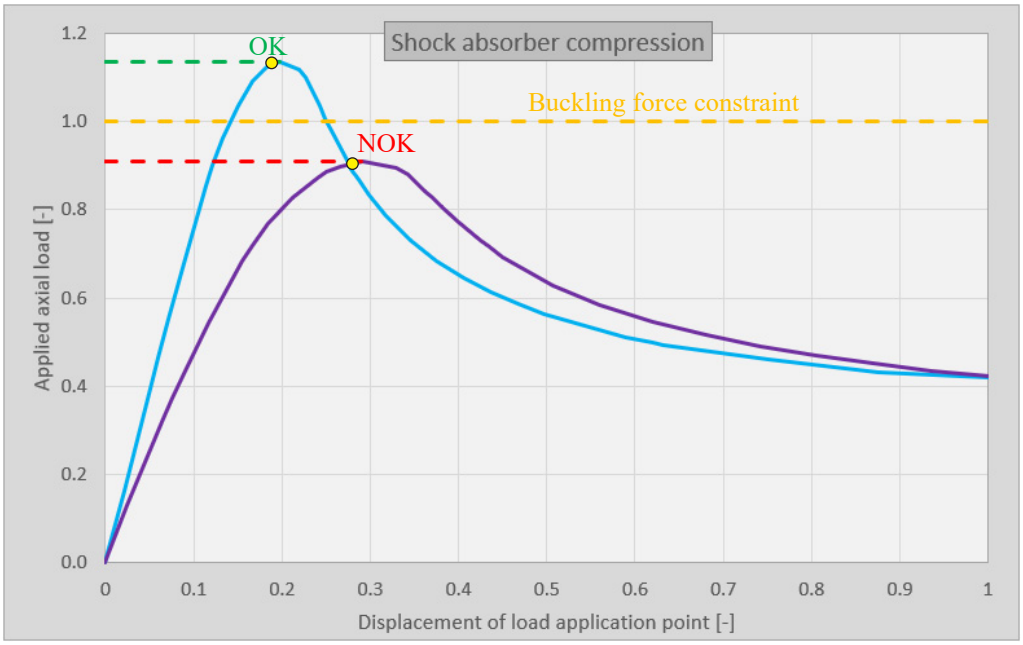

Fig. 3. Exemplary load-deflection curves for design meeting the minimum buckling force constraint (blue) and design violating this constraint (violet). Forces and displacements are presented as values relative to the maximum used in similar applications

The second point is associated with one of the main difficulties in gradient-based methods, which is the determination of a starting point. In such a case, the randomness of, e.g., evolutionary algorithms helps to achieve the feasible solution when it is hard to obtain any shape due to implicit geometry representation.

The resultant shape of the bracket (or any optimized part in general) is a result of the distribution of the auxiliary field values. For each of the finite element centroid, the auxiliary field value is calculated:

$$\Phi = \sum_{i=1}^{N} KV_i \varphi_i(\|\mathbf{x} - \mathbf{x_i}\|) \tag{3}$$

where: Φ – auxiliary field value, φ_i – shape function, $\mathbf{x}$ – finite element centroidal coordinates vector; $\mathbf{x_i}$ – interpolation knot coordinates vector, N – total number of interpolation knots;

and compared with the threshold:

$$\begin{cases} \Phi \geq threshold \rightarrow material \\ \Phi < threshold \rightarrow void \end{cases} \tag{4}$$

where the shape function is realized by the Gaussian-based radial basis function:

$$\varphi_i(\|\mathbf{x} - \mathbf{x_i}\|) = e^{\frac{\|\mathbf{x}-\mathbf{x_i}\|^2}{d}} \tag{5}$$

where d is the average distance between the interpolation knots grid.

Therefore the optimization problem may be reformulated as:

$$f(KV_1, KV_2, ..., KV_N, threshold) = \rho \int_V dV \rightarrow \rho \sum_{i=1}^{N} V_i \tag{6}$$

subjected to:

$$g(KV_1, KV_2, ..., KV_N, threshold) \geq F_{LIMIT} \tag{7}$$

One of the challenges associated with the reduced parameter level-set method is the sufficient resolution of the geometry representation. With an increasing number of parameters, the resultant geometry can be better represented in terms of small features and details, like the smoothness of transitions between neighboring surfaces. At the same time, it is much harder to obtain a feasible starting point, as the increased number of parameters combination makes it challenging to create a feasible design with a random search (as in the case of the genetic algorithm). On the other hand, a lower number of parameters increase the convergence rate of the problem and therefore reduces the computational cost of the optimization by lowering the amount of the objective function calls. The auxiliary field interpolation is based on the interpolation knots distribution presented in Figure 4. The knots allocation presented below is based on the cross-sectional area of the bracket at the height of the interpolation knots planes, which are distributed over the height of the bracket in a semi-regular manner. The planes at which knots are located (there are five such planes, as presented in Figure 4b) match the inclinations and shape of the design area.

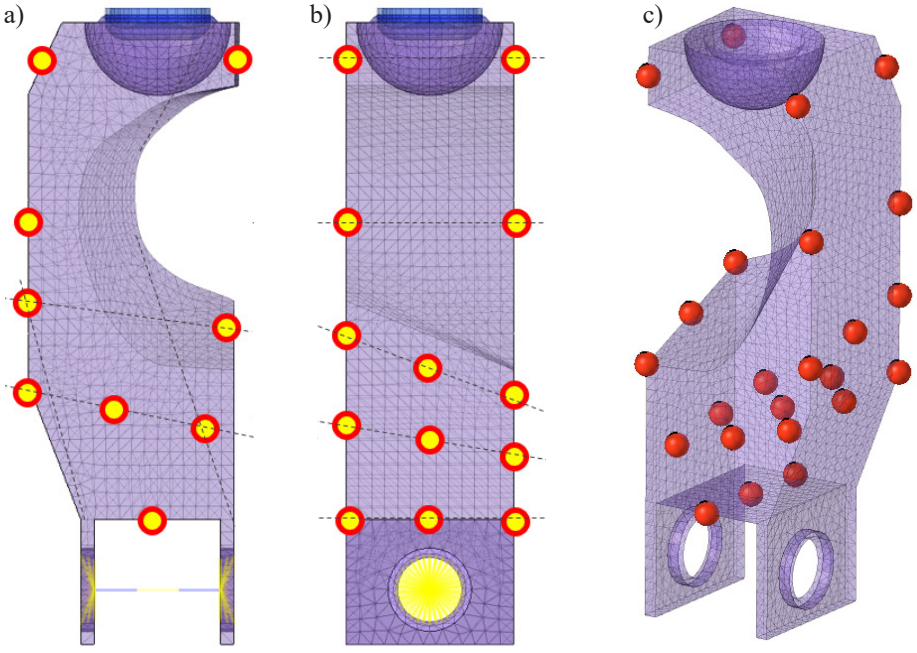

Fig. 4. The distribution of the interpolation knots in the first model over the design area: a) XZ view; b) YZ view; c) semi-isometric view

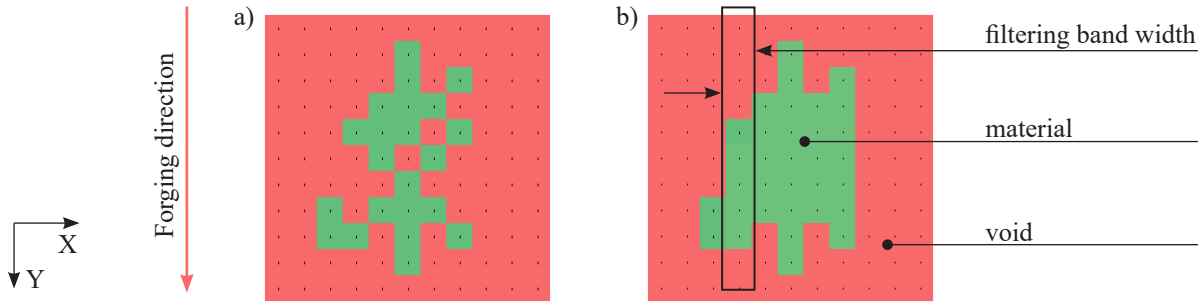

Fig. 5. The schematic representation of the material filtering. The cross-sectional view of the part: a) after the optimization iteration; b) after applying the manufacturability filter

3.2. Filtering – the condition of manufacturability

In order to greatly increase the manufacturability of the resultant bracket geometry, the filtering routine was implemented in the optimization algorithm. The filters sequence of actions is following:

- division of the bracket into regions;
- application of the incremental cross-sectional auxiliary field scanning over the height of the bracket;
- for each of the given cross-sections, the elements on the boundary (considering the forging directions) with $\Phi \geq threshold$, are saved into algorithms memory;
- each void-marked element with $\Phi < threshold$ laying between the saved elements is filled with the material.

A schematic representation of the filter is shown in Figure 5, for one random cross-section. The forging direction is aligned with the Y-axis presented in Figure 1.

3.3. Optimization algorithms

In order to solve the complex optimization task, two groups of algorithms were used:

- stochastic algorithms:
  - multi-island genetic algorithm (MIGA),
  - evolution strategy (EVOL),
- deterministic algorithm:
  - nonlinear programming by quadratic Lagrangian (NLPQPL).

The version of the MIGA used in the optimization is the extension of the classic genetic algorithm (Whitley et al., 1999). The improvement was made, as (comparing to the initial approach presented by J. Holland back in 1975) the MIGA consists of several independent islands at which autonomous (random) populations are created at the first stage of the algorithm. The rest of the operators are the same as in the classic approach (crossover, mutation, elitism) with one distinction – additional migration occurs every n_{migr_MIGA} generation with the probability p_{migr_MIGA}. In such a case, the evolution process is not dominated by the particular best-fitted individual from initial generations, and more diversity is employed.

The second biology-inspired algorithm is evolution strategy (EVOL) inspired by the works of Rechelnberg, and Beyer and Schwefel (2002), even though Fogel is considered as the father of evolutionary methods in general. What makes it different from the classical genetic algorithm is the fact, that each offspring is generated only by mutation, and each generation consists of only one offspring. The mutation is controlled by a randomly added value, chosen according to Gaussian normal distribution. The process is self-adaptive, as the range of mutation is modified based on the fitness function of the m previous mutants (offsprings).

On the other hand, the gradient-based method called "nonlinear programming by quadratic Lagrangian" represents the group of deterministic algorithms. This method is a quasi-Newton version of gradient algorithm, which uses the BFGS method to update the Hessian of the Lagrange function and linear approximation of output constraints (Shittkowski, 1986; Shittkowski et al., 1994). Gradients are calculated by the forward or backward difference method, and for each iteration, more than one gradient point might be used for each of the design variables, which is particularly useful at the first iteration of the algorithm (due to the quadratic nature of the approximation of Lagrange function).

The algorithms listed above were chosen based on their advantages, i.e., randomness incorporated in biology-inspired algorithms and capability of finding the true optimum associated with the gradient-based algorithms. As the determination of starting point is a critical part of the gradient search, the NLPQPL method was started from the feasible point obtained during the MIGA operation, creating the hybrid optimization method (Burczyński & Orantek, 1999; Burczyński et al., 2020).

Additionally, the combination of the algorithms described above was introduced into the optimization flow. The hybrid attitude consisted of subsequent optimization scenarios, where each scenario is started from the best individual obtained from the previous task. Only the genetic algorithm is using random search to obtain the first generation. The schematic representation of such an algorithm is presented in Figure 6.

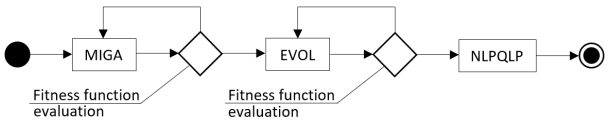

Fig. 6. The hybrid optimization flow

4. Results

An optimization process was conducted for the whole shock absorber model (system-based approach), and the maximum achieved force at the maximum load capacity was recorded in each of the design iterations. The first model consisted of 28 design parameters, from which 27 controlled the auxiliary field (by changing the weights assigned to the interpolation knots) and one parameter was controlling the threshold directly. The analysis of results for the first model, without the filtering routine implemented, was started from the first MIGA generation. It was observed, that there were many (over 50%) designs that were not meeting the limit force constraint, from which almost 15% were not even feasible designs at all (i.e. those designs were internally unconnected). Such a situation is presented in Figure 7 below. It is critical for the brackets functionality, to have both sides connected via the bolt connection. Any design that does not meet this requirement, or violates the manufacturability conditions, is assumed as infeasible.

Even though the first generation consisted of many infeasible individuals, the total amount of such design points were almost entirely eliminated through the evolution process, due to the strong penalization of severely unfitted individuals. On the other hand, after the first generation, the number of designs violating the limit force constraint was lowered at the beginning stage of the MIGA. Starting from the 4th generation, the occurrence frequency of the weak designs started to grow, as many designs oscillated around the required limit load. The change of both indicators is presented in Figure 8.

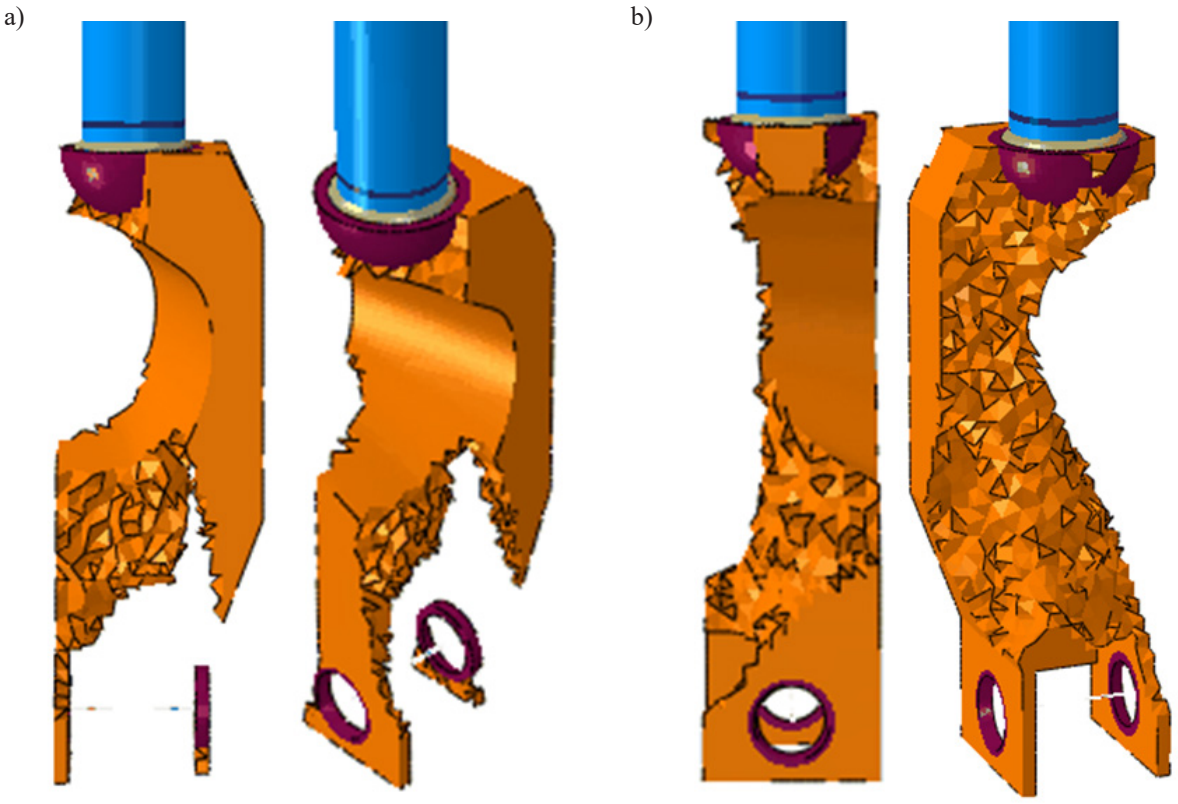

Fig. 7. Two extreme representants of the MIGA first generation: a) unconnected design; b) feasible design fulfilling the buckling force constraint

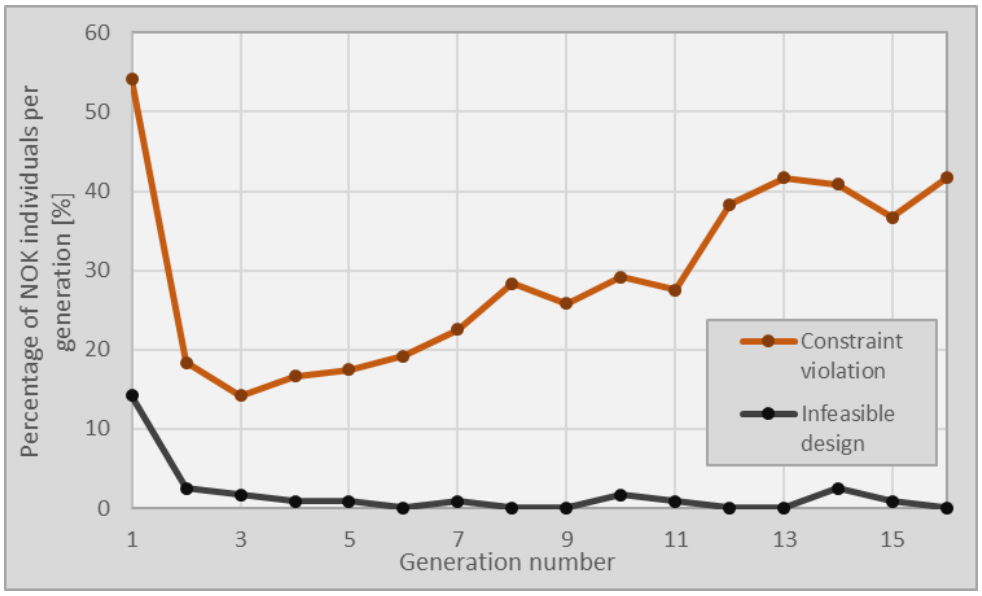

Fig. 8. The participation factors [%] of infeasible designs (black) and designs violating the buckling force constraint (brown) over the MIGA generations

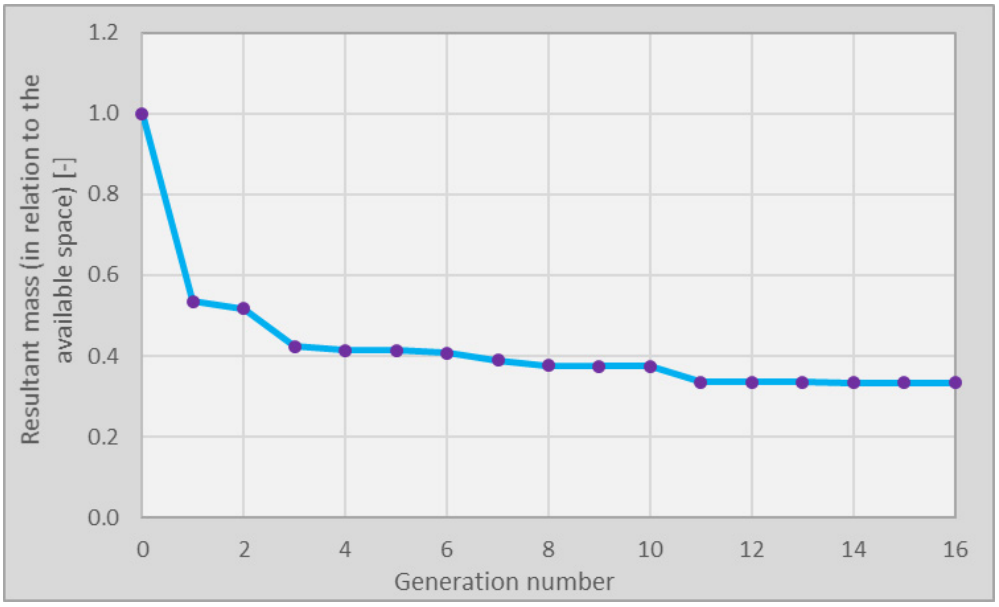

Fig. 9. The objective function as a function of MIGA generations

The objective function convergence plot of the MIGA optimization is shown in Figure 9. A major mass decrease is realized after the first generation due to random search. In the subsequent generations, over 65% of the initial mass is eliminated from the model. However, the objective function was changed by less than 0.5% from 11th to the last, 16th generation. The final best-fitted individual had the resultant mass of 0.33 (where 1.0 mass is equivalent to the whole design area). Nevertheless, poor connectivity was observed, making the design moderately useful for the forging process (Fig. 10).

In order to increase the quality of the optimization result, a second optimization attempt was initiated using a gradient-based search. As the determination of the starting point is critical for such a group of algorithms, one of the mid-generation feasible solutions from the MIGA process was used. Even though the resultant bracket geometry is similar to the one obtained in the MIGA, the new design is free from the connectivity issues observed in the first optimization attempt. The shape of the initial and the last iterations are presented in Figure 11.

Fig. 10. The best-fitted individual from the MIGA last generation

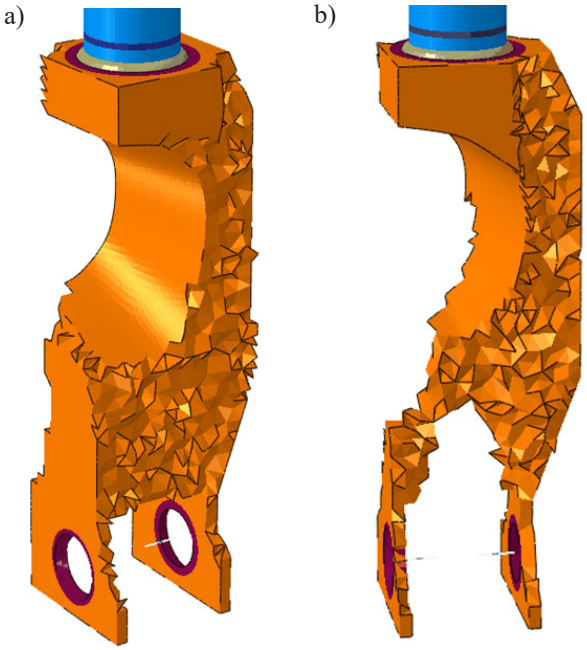

Fig. 11. The shape of the bracket for: a) initial (starting point); b) the last iteration of the NLPQLP algorithm

The evolution of the brackets mass as a function of gradient-based NLPQLP optimization iteration is shown in Figure 12. In total, the process consisted of 35 iterations, however, there were only minor objective function improvements after the 20th iteration. The resultant mass of the part is 0.39, comparing to 0.33 obtained from the MIGA optimization. On the other hand, the increase in the feasibility was noticed, even though the mass reduction potential is still observed (unstressed regions).

Due to the manufacturability issues of the first model, the second optimization strategy was started with some modifications implemented. First of all, the quantity (and therefore location) of interpolation knots was increased, to achieve a better geometrical representation of the FEM model, as presented in Figure 13.

Secondly, the number of generations in the MIGA decreased from 16 to 10, and the number of individuals per island from 12 to 10. The number of islands was held constant (10). As a result, the optimization flow changed, making it possible to involve one additional biology-inspired algorithm – EVOL. It was used as the middle stage of the optimization process, after which the gradient-based search was initiated.

The reason for implementing the additional algorithm was that the distributed genetic algorithm (MIGA) works well for highly nonlinear and design spaces, but it tends to produce only a few individuals around the optimal point. The evolution strategy (EVOL) is able to search the neighborhood of the so-far the best individual, without converging into local minima as the gradient-based algorithms do. Since the intensity of the mutation is adjusted to the change in the objective function, EVOL may find an alternative optimal point, which is no longer associated with the previously found "best so far" point. The gradient-based optimization (NLPQLP) is able to converge to the actual optima (regardless of local or global case), without a noise generated by randomly-added variations (like mutation). The effect of such combined (hybrid) optimization is shown on the convergence plot in Figure 14. The EVOL generations are presented schematically, as a result is plotted for each 20th offspring (even though in total there were 200 mutants in total, each one is considered as a separate generation).

Similar to the first optimization described in this paper, the first significant mass decrease is achieved just due to random search in the first MIGA generation. Subsequent generations provide an additional 8% mass reduction (total of 1000 function calls). The best-fitted individual from the distributed genetic algorithm was automatically chosen as the initial parent for the evolution strategy. After generating 200 subsequent mutants by the EVOL, the brackets mass was furtherly lowered by 7%. The final mass decrease was achieved by the NLPQLP algorithm, which found the optimized shape using three gradient-based search iterations. The resultant decrease in mass was achieved at the level of 0.41, which is very similar (2% difference) to the NLPQLP result of the first optimization model.

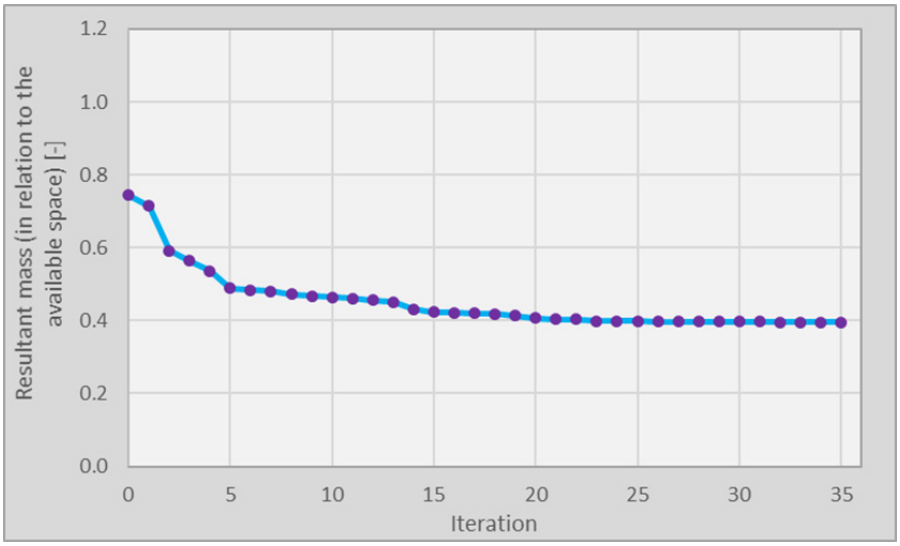

Fig. 12. The objective function as a function of NLPQLP iterations

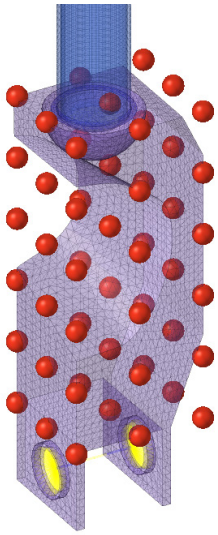

Fig. 13. The distribution of the interpolation knots over the design area for the second optimization model

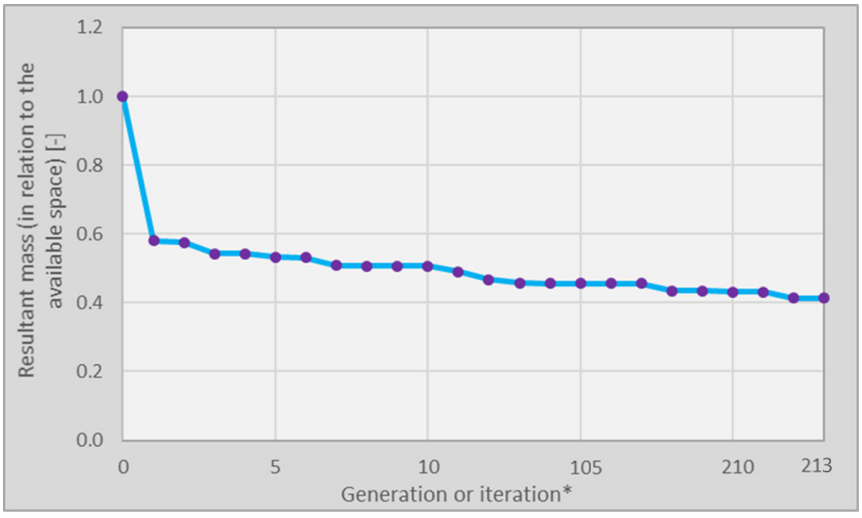

Fig. 14. The objective function as a function of MIGA & EVOL generations and NLPQLP iterations

The resultant shapes at each of the optimization flow stages are shown in Figure 15. It is important to notice, that even though the material filtering was implemented, the final structure again suffered from feasibility issues (discontinuous material distribution marked with red squares). Such features could be eliminated by increasing the filtering band width, on the cost of the accuracy of the geometrical features representation.

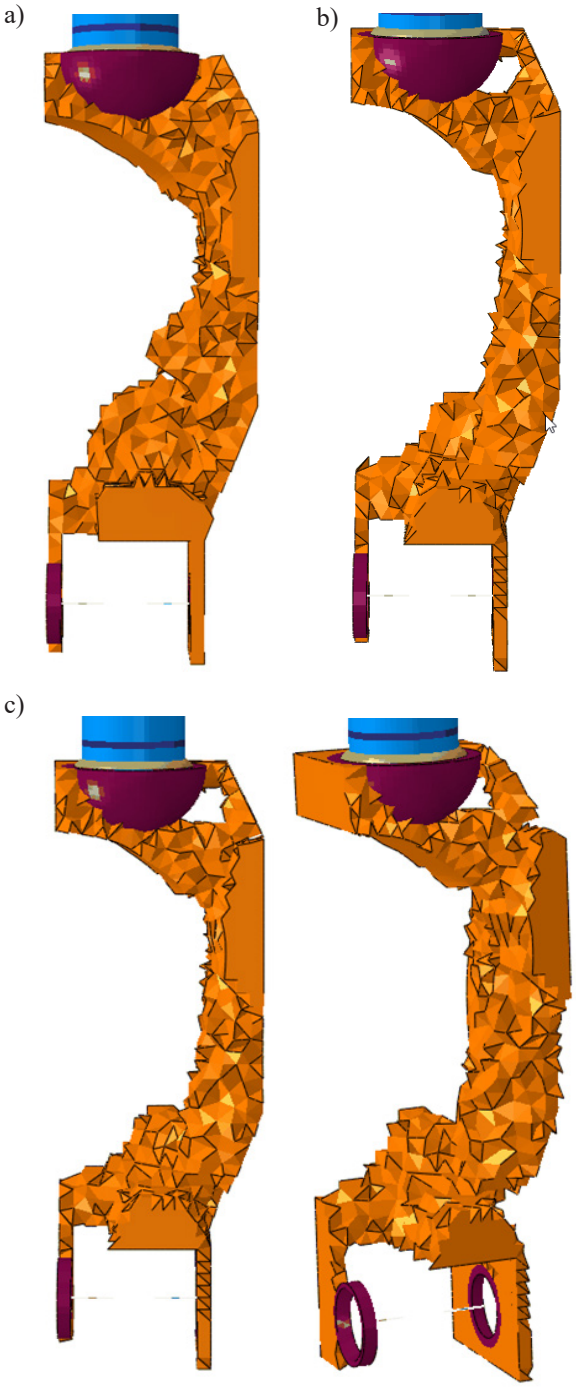

Fig. 15. The resultant shapes for each of the optimization phases: a) the best fitted MIGA individual; b) the best fitted EVOL individual; c) the final, optimized shape after the NLPQLP algorithm

5. Discussion

The proposed optimization method – the level-set-based method using finite element analysis, was able to solve the highly nonlinear optimization task presented. In the current version of the method, there is a possibility to create an infeasible design. That is why authors aim to resolve those issues by implementing material distribution filtering routines and/or applying different optimization algorithms. As the calculations have shown, more sophisticated algorithms are needed to resolve the feasibility issues, or on the contrary, lower filter resolution (filtering band width) may be used to mitigate the effect of discontinuous material distribution.

Using random search to create the first individuals in the genetic algorithm, many of the created designs were unconnected or had poor connectivity. Such phenomenon may be resolved by adding additional filtering or using selection even in the first generation (i.e. excluding the infeasible designs to achieve a more diverse, yet feasible generation). Regardless of the number of infeasible designs at the beginning of the genetic algorithm, subsequent generations consisted almost exclusively of feasible solutions. That was achieved by the severe penalization of designs with insufficient connectivity.

As shown in the second optimization model, adding the evolution strategy as the mid-step in the optimization process, helped to reduce the mass using only 200 function calls (comparing to 1000 for the MIGA and over 100 for the NLPQLP). It can be recognized as a compromise between the global genetic algorithm and local gradient-based search using only a moderate amount of the FEM solver calls. What is also important is the fact, that even though the gradient-based search seemed very effective (over 2% mass reduction in 3 iterations), the total number of finite element analysis is still high, as the determination of search direction, using finite difference approach is linearly dependent on the number of design parameters. This is even more computationally expensive, when two gradient points are used, which is useful in particular in the first iteration of the gradient calculations, as the Hessian matrix is better represented (comparing to the identity matrix) at the beginning of the NLPQLP operation.

The proposed methodology may be applied to other fields of engineering such as civil engineering, especially if the optimization concerns the unstable behavior of the part or assembly. Nonetheless, the combination of implicit geometry representation (as in the proposed level-set method) and material filtering (for assuring the feasibility) creates a universal optimization tool which can be used regardless of the shape or size of the optimized part.

Acknowledgments

The research was co-financed under the grant no DWD/3/7/2019 supported by the Ministry of Science and Higher Education in Poland and research subsidy of the Mechanical Engineering Faculty, Silesian University of Technology.

References

Bendsøe, M. (1989). Optimal shape design as a material distribution problem. *Structural Optimization*, *1*(4), 193–202.

Beyer, H.-G., & Schwefel, H.-P. (2002). Evolution strategies – A comprehensive introduction. *Natural Computing*, *1*(1), 3–52.

Burczyński, T., & Orantek, P. (1999). Coupling of genetic and gradient algorithms. In *Proceedings of Conference on Evolutionary Algorithms and Global Optimization* (pp. 112–114).

Burczyński, T., Kuś, W., Beluch, W., Długosz, A., Poteralski, A., & Szczepanik, M. (2020). *Inteligent Computing in Optimal Design*. Springer International Publishing.

Ferrari, F., & Sigmund, O. (2020). Towards solving large-scale topology optimization problems with buckling constraints at the cost of linear analyses. *Computer Methods in Applied Mechanics and Engineering*, *363*, 112911.

Guirguis, D., & Aly, M. (2016). A derivative-free level-set method for topology optimization. *Finite Elements in Analysis and Design*, *120*, 41–56.

Hongwen, H., Lu, Y., & Peng, J. (2017). Combinatorial optimization algorithm of MIGA and NLPQL for a plug-in hybrid electric bus parameters optimization. *Energy Procedia*, *105*, 2460–2465.

Hu, X., Chen, X., Zhao, Y., & Yao, W. (2014). Optimization design of satellite separation systems based on Multi-Island Genetic Algorithm. *Advances in Space Research*, *53*, 870–876.

Li, H., Li, P., Gao, L., Li, Z., & Wu, T. (2015). A level set method for topological shape optimization of 3D structures with extrusion constraints. *Computer Methods in Applied Mechanics and Engineering*, *283*, 615–635.

Ntintakis, I., Stavroulakis, G., & Plakia, N. (2020). Topology Optimization by the use of 3D Printing Technology in the Product Design Process. *HighTech and Innovation Journal*, *1*(4), 161–171.

Schittkowski, K. (1986). NLPQLP: *A Fortran Implementation of a Sequential Quadratic Programming Algorithm with Distributed and Non-Monotone Line Search*. User's Guide, Version 4.2.

Schittkowski, K., Zillober, C., & Zotemantel, R. (1994). Numerical comparison of nonlinear programming algorithms for structural optimization. *Structural Optimization*, *7*, 1–19.

Stolpe, M., & Svanberg, K. (2001). An alternative interpolation scheme for minimum compliance topology optimization. *Structural and Multidisciplinary Optimization*, *22*(2), 116–124.

Vatanabe, S.L., Lippi, T.N., Lima, C.R., de, Paulino, G.H., & Silva, E.C.N. (2016). Topology Optimization with Manufacturing Constraints: A Unified Projection-Based Approach. *Advances in Engineering Software*, *100*, 97–112.

Wang, S., & Wang, M.Y. (2006). Radial basis functions and level set method for structural topology optimization. *International Journal for Numerical Methods*, *65*(12), 2060–2090.

Whitley, D., Rana, S., & Hackendorn, R.B. (1999). The Island Model Genetic Algorithm: On Separability, Population Size and Convergence. *Journal of Computing and Information Technology*, *7*(1), 33–47.

Zhou, M., Shyy, Y.K., & Thomas, H.L. (2001). Checkerboard and minimum member size control in topology optimization. *Structural and Multidisciplinary Optimization*, *21*(2), 152–158.